



HAL
open science

Solar thermo-hydraulic engine for combined heat, cold and electricity production for the residential sector

Remy Borgogno, Gilles Marck, Mauran Sylvain, Driss Stitou

► To cite this version:

Remy Borgogno, Gilles Marck, Mauran Sylvain, Driss Stitou. Solar thermo-hydraulic engine for combined heat, cold and electricity production for the residential sector. 28th Int. Conf on Efficiency, Cost, Optimization, Simulation, ECOS 2015, Jun 2015, Pau (FRA), France. hal-04818244

HAL Id: hal-04818244

<https://cnrs.hal.science/hal-04818244v1>

Submitted on 4 Dec 2024

HAL is a multi-disciplinary open access archive for the deposit and dissemination of scientific research documents, whether they are published or not. The documents may come from teaching and research institutions in France or abroad, or from public or private research centers.

L'archive ouverte pluridisciplinaire **HAL**, est destinée au dépôt et à la diffusion de documents scientifiques de niveau recherche, publiés ou non, émanant des établissements d'enseignement et de recherche français ou étrangers, des laboratoires publics ou privés.

Solar thermo-hydraulic engine for combined heat, cold and electricity production for the residential sector.

Rémy Borgogno^{ab}, Gilles Marck^{bc}, Sylvain Mauran^{ab} and Driss Stitou^b

^a *Université de Perpignan Via Domitia (UPVD), Perpignan, France,
remy.borgogno@promes.cnrs.fr ; mauran@univ-perp.fr*

^b *Laboratoire PROMES-CNRS, UPR 8521, Perpignan, France,
stitou@univ-perp.fr*

^c *AxLR SATT, Montpellier, France,
Gilles.MARCK@axlr.com*

Abstract:

This article presents a solar driven thermo-hydraulic system actuated by the low-grade solar thermal energy produced by flat plate solar collectors. This solar process aims at providing heat or cold production or electricity generation. This innovative system is made of two integrated thermo-hydraulic processes: a CHV3T sub-system that ensures the cold or heat production and a CAPILI sub-system dedicated to the electricity generation. The CHV3T sub-system is a trithermal process resulting from the combination of two dithermal systems, the motor cycle producing work to drive the receiver cycle who produced cold or heat. The dithermal systems operate with different working fluids and are mechanically coupled with an hydraulic process, that is a transfer liquid acting as a liquid piston. The engine cycle is used to convert the low-temperature driving heat into hydraulic energy that is transferred to the liquid piston within a transfer cylinder. The receiver cycle uses this hydraulic energy, provided by the liquid piston, to perform the compression step of the refrigerating cycle. In the frame of domestic use, the engine and refrigerating dithermal cycles allow producing either a subsequent amount of cold at the evaporator of the receiver cycle, or a larger amount of heat by means of the condensers of the receiver and engine cycles. When cooling or heating needs are not required, the receiver sub-system cycle of the CHV3T is isolated and the engine cycle operates as a CAPILI cycle in order to drive a Francis-type hydraulic turbine for electricity generation.

A quasi-static model of the whole system is developed in order to define the best operating conditions. The results enable the selection of the best couple of working fluids for production of heat, cold and electricity, with preferably low GWP working fluids. In addition, a parametric study helps to design the hydraulic Francis-type turbine that is required for a small-scale pilot of 1kWel.

Keywords:

Low temperature thermal solar conversion; Thermo-hydraulic cycle; Micro-cogeneration.

1. Introduction

The main conclusion highlighted by the 5th report of the "IPCC" (Intergovernmental panel on climate change) point out that a global temperature increase, exceeding 2°C, would have dramatic and irreversible consequences on the environment [1]. The residential and tertiary sectors are the most consuming sectors in Europe with more than 40 % of the consumed final energy and more of 20% of the GHG (Greenhouse gas) emission. Therefore, both sectors draw attention in the recent EU 2030 framework for climate and energy policies, which aims at reducing of the GHG emission by 40% and increasing the part of clean energies and energy efficiency by 27% [2]. One solution is to replace the fossil fuels that are widely used in the residential sector by renewable energy sources in order to meet the various domestic needs, such as heat, cold, and electricity. Another method tackles the efficiency of the current systems. Co-generation and tri-generation systems can take advantages of these both approaches for satisfying efficiently and wisely these residential needs.

1.1 – State of the art

The trigeneration systems (heat, cold and electricity) are still weakly developed in the residential sector, but mCHP (micro combined heat and power) are increasingly developing into the housing sector. Several technologies are already on the market, such as the reciprocating internal combustion engine, the fuel cell, the micro-turbine, the Stirling engine or the ORC cycle (organic Rankine cycle) [3], [4]. The heat source of these technologies is mostly ensured by fossil fuels. Some applications using renewable energy are still under development and they do not have reached the required technological maturity for their commercialization [5]. However some systems using biomass-generated heat source start gaining market shares.

The cold production from renewable energies relies on different technologies, like absorption and adsorption process, thermochemical systems, Vuilleumier-Stirling system or the combined organic Rankine cycle [6]. All these processes remain at an experimental level; only absorption systems really started its market penetration.

Some solutions mentioned above begin to be studied for trigeneration systems but none of them give rise to a potentially commercial application. Linking PV panels with reversible heat pumps remains the closest way to achieve trigeneration with standard industrial components. The continuous increase of the energy pricing would shortly lead to make these two technologies economically competitive for new cogeneration and trigeneration applications.

Although few studies deal with thermo-hydraulic systems, some firms investigate this field and have registered several patents [7] [8]. Thermo-hydraulic processes could be an original solution for the heat/cold and electric production: its high exergetic efficiency is particularly suited for exploiting the low temperature heat sources like the OTEC (Ocean Thermal Energy) or flat plate collectors.

2. Principle of thermal-hydraulic process

Thermo-hydraulic processes are based on the transformation of thermal energy into work by using an hydraulic compression of fluid. The trigeneration process studied through this article deals with two sub-systems. On the one hand, the work produced by the working fluid expansion can be used to produce electricity throughout a hydraulic turbine: this process is referred as CAPILI [9] [10] and is cheaper and more robust than a vapor turbine. On the other hand, another thermodynamic machinery, called CHV3T [11], can be composed by putting together two thermodynamic processes operating in phase opposition to produce heat or cold heat fluxes. The main advantage of both processes lie on efficient heat exchanges between the different heat sources/sinks since those rely on liquid/vapor phase change of the fluids. They also lead to a better thermodynamic efficiency since the cycle irreversibilities are reduced: no vapor overheating is required at the evaporator outlet, contrary to the state of vapor entering the turbine in ORC systems in order to avoid damaging its bladings.

The CHV3T process have the advantage to carry out simple and cheap industrial components, which allow limiting the system cost: an evaporator (E), a condenser (M), a receiver (BS), a pump (P) and a hydraulic turbine (HT). The only parts that do not exist are transfer cylinders (CT), although hydraulic accumulators can replaced them. The subscript (R and M) on inch component indicate receiver and motor.

The following figure shows how to pair CHV3T sub-system (the left hand side part is the receiver cycle and the right hand side part is the motor cycle) and CAPILI subsystem, which add an hydraulic turbine to CHV3T subsystems in order to convert hydraulic works between CT_M and $CT_{M'}$ into electricity.

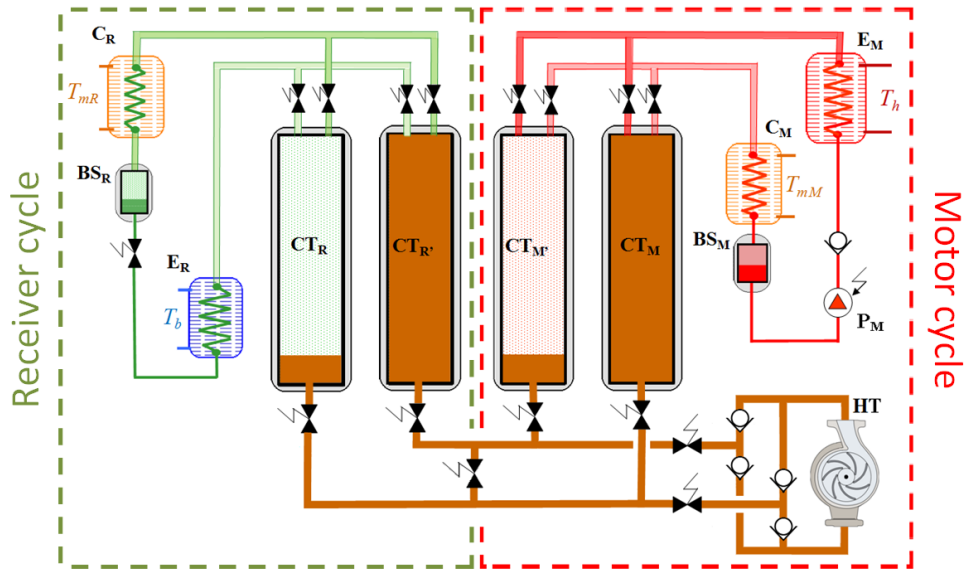


Fig. 1. Scheme of integrated CHV3T- W_L and CAPILI cycles

2.1. CHV3T cycle

The CHV3T system has been already described in details in a previous article [10], as a trithermal machine that exchange heat at three different levels of temperature. In cooling mode, hot temperature (T_h) is set by the solar collectors, intermediate temperature (T_m) match with ambient temperature and low temperature (T_b) corresponds to the cold production temperature.

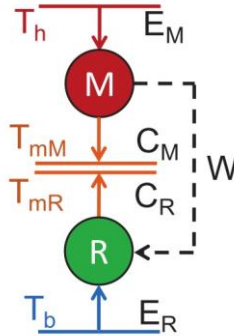


Fig. 2. Schematic diagram of the coupling between two dithermal machines.

Several variants of the CHV3T process exist, with different level of complexity. The simplest one, called CHV3T- W_0 , uses only two transfer cylinders that are periodically connected to the different components (evaporator and condenser) or isolated from the other parts of the system. This operating mode increases drastically the thermodynamic irreversibilities during some phases of the cycle, that is to say the pressurization phases. To prevent these phenomena, the process operates by using four transfer cylinders, enabling to run two W_0 cycles in phase opposition. In this way, the evaporator and condenser are always used and connected to the cylinders leading to a reduction of irreversibilities.

When two W_0 cycles are used in phase opposition, it is possible to implement an additional phase (ϵ) aiming at recovering the high-pressure energy stored within one of the motor transfer cylinders to compress the receptor fluid. On this variant, called CHV3T- W_L , the energy is recovered via the hydraulic liquid as an additional work. Another variant, denoted CHV3T- W_G , may also recover energy, but from the working fluid under its gaseous phase.

These two enhancements can also be add up on two new variants CHV3T- W_{LG} or CHV3T- W_{GL} but these both solutions are not a suitable trade-off between their efficiency gain and their industrial complexity.

2.2. CAPILI cycle

The CAPILI concept aims at converting heat in electricity with high exergetic efficiency, defined as the ratio of energetic efficiency by the Carnot efficiency. In this process, the work produced by the vapor expansion in the cylinder is passed to the transfer fluid, which set into motion an hydraulic turbine. Therefore, the expansion work is used by an hydraulic turbine, instead of a vapor one which is usually used in ORC systems and are characterized by low isentropic efficiency (60-70%) [12]. The hydraulic turbine can reach a better efficiency of the hydraulic/mechanic/electric conversion chain, if the phases where it operates under variable pressure differences not penalize the efficiency.

In a similar way of the CHV3T subsystem, the CAPILI process does not need any overheating at the end of the evaporation phase, neither subcooling at the end of condensation phase. Two different variants of the CAPILI cycle exist, but the second one is far too complex to consider using it in the frame of a domestic electricity production purpose. The CAPILI cycle is more detailed in the following article [9]

3. Steady state study

The steady state study aims at evaluating the system performances under stationary conditions. Using simplifying assumptions, the performances of each cycle can be evaluated and compared with the existing technologies under the same operating conditions. This study will also estimate which pair of working fluids is the most suitable regarding efficiency matters, and will trigger the design of the main components. The simplifying assumptions are the following ones:

- Potential and kinetic energy variations are neglected
- Thermal inertia of components is neglected
- Pump and turbine efficiencies are equal to unity
- No pressure drop between the different components

3.1. Preliminary calculation

The different efficiencies of the process depend on the heat source and sink temperatures, which also depend on solar collector and heat exchangers characteristics.

3.1.1. Flat plate collector efficiency

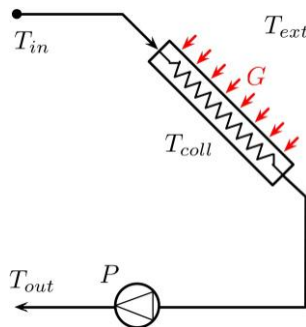


Fig. 3. Model of solar collector.

The solar collector efficiency is governed by the following equations:

$$\eta_{coll}(T_{coll}, T_{ext}, G) = \eta_0 - k_1 T^* - k_2 G T^{*2} \quad (1)$$

Where η_0 The optical efficiency

k_1 The linear thermal loss coefficient ($Wm^{-2}K^{-1}$).

k_2 The quadratic thermal loss coefficient ($Wm^{-2}K^{-2}$).

G The solar irradiance (W/m^2).

$$T^* = \frac{T_{coll} - T_{ext}}{G} \quad (2)$$

$$T_{coll} = \frac{T_{in} + T_{out}}{2} \quad (3)$$

The efficiency of a solar collector can be known for any heat source temperature, if the parameters η_0 , k_1 and k_2 are known: those have been provided by the ‘‘Solar keymark’’ website [13]. If the heat source temperature is too high, and even if it allows increasing the cycle thermodynamic efficiency, it leads to decrease the solar collector efficiency. Consequently, the selection of both solar collector model and the working fluids strongly depends on the CHV3T variant selected.

3.1.2. Heat exchanger model

The high and low temperatures of thermodynamic cycles are set by the surrounding temperatures. Consequently, a generic model of heat exchangers is required in order to compute the heat and cold source temperatures. Those are modeled thanks to a constant efficiency (0.7 for ϵ_{gl} and 0.65 ϵ_{ll}) and a given temperature pinch (1,5°C). These both parameters allow evaluating the average temperature T_{coll} of the heat transfer fluid inside the solar collector from the operating conditions.

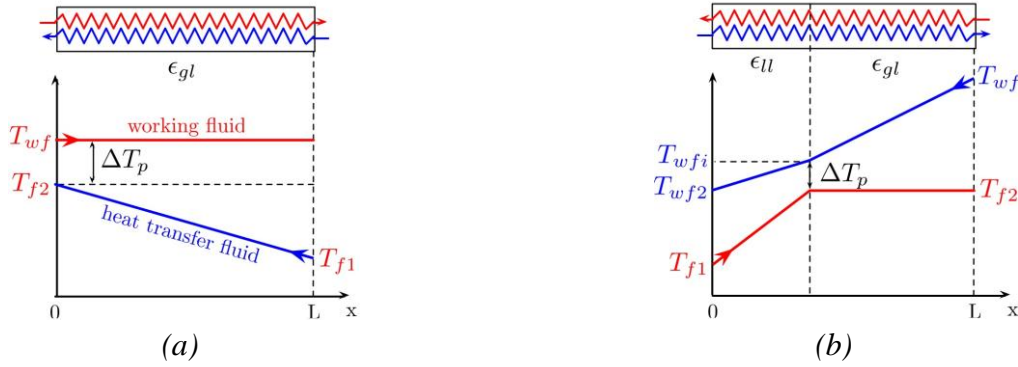


Fig. 4. Model of condenser (a) and evaporator (b).

The following equations described the thermal behaviour of the condenser:

$$T_{wf} = T_{f2} + \Delta T_p \quad (4)$$

$$T_{wf} = T_{f1} + \frac{\Delta T_p}{1 - \epsilon_{gl}} \quad (5)$$

The liquid/vapour phase change in the evaporator requires the use of two different heat exchanger efficiencies, one for the liquid part and one for the vapour part, in addition to the temperature pinch. Therefore, the evaporator behaviour is described thanks to:

$$T_{wfi} = T_{f2} + \Delta T_p \quad (6)$$

$$T_{wf} = \frac{T_{wfi} - \epsilon_{gl}T_{f2}}{1 - \epsilon_{gl}} \quad (7)$$

$$T_{wf2} = (1 - \epsilon_{ll})T_{wfi} + \epsilon_{ll}T_{f1} \quad (8)$$

Knowing the different temperatures allow to deducting the pressures P_h and P_b (high and low pressure) for a given fluid.

3.2. CHV3T

3.2.1. Basic performance evaluation of CHV3T process

Once the internal temperatures of the cycle have been set, the intensive thermodynamic properties of the working fluids can be computed thanks to a thermodynamic database. RefProp and CoolProp libraries have been used to determine pressure, density, volume, enthalpy, entropy or quality factor of each point of the two cycles described below.

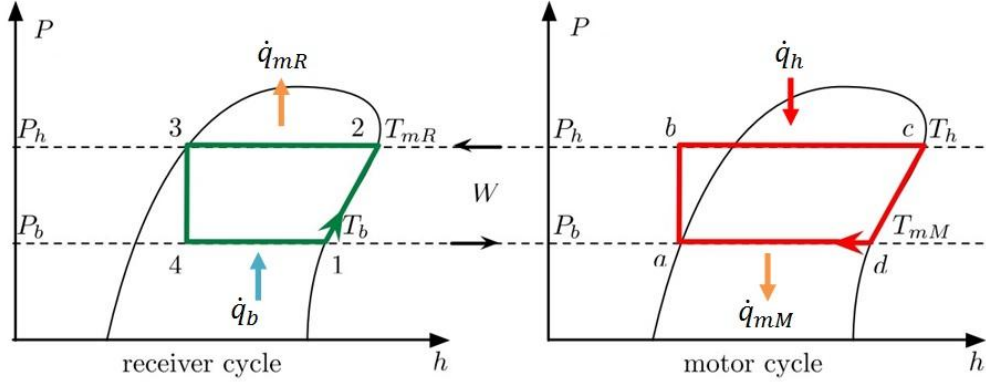


Fig. 5. Motor and receptor Mollier diagram of CHV3T cycle in W_0 variant.

The coefficient of performance (COP), defining the efficiency of cold production, and the coefficient of amplification (COA), defining the efficiency of the heat production, can be computed for a large range of working fluid pairs. In addition, the exergetic efficiency of the system can be evaluated from COP, COA and Carnot efficiency values. This last criterion describes the thermodynamic gap of the system from an ideal reference. The following equations described the different COP and COA coefficients.

COP Calculation:

$$COP_{Carnot}^{W_0} = COP_C^{W_0} = \frac{T_b(T_h - T_{mM})}{T_h(T_{mR} - T_b)} \quad (9)$$

$$COP_{th}^{W_0} = \frac{\dot{q}_b}{\dot{q}_h + \dot{w}} = \frac{v_c^n(h_1^n - h_4^n)}{v_1^n(h_c^n - h_a^n)} \quad (10)$$

$$COP_{ex}^{W_0} = \frac{COP_{th}^{W_0}}{COP_C^{W_0}} \quad (11)$$

COA Calculation:

$$COA_C^{W_0} = 1 + COP_C^{W_0} \quad (12)$$

$$COA_{th}^{W_0} = \frac{\dot{q}_{mR} + \dot{q}_{mM}}{\dot{q}_h + \dot{w}} = \frac{n_{c \rightarrow a}(h_c^n - h_a^n) + n_{2 \rightarrow 3}(h_2^n - h_3^n) - n_{1 \rightarrow 2}(h_2^n - h_1^n)}{n_{c \rightarrow a}(h_c^n - h_a^n)} \quad (13)$$

With:

$$n_R = n_{1 \rightarrow 2} = n_{2 \rightarrow 3} \quad (14)$$

$$h_3^n = h_4^n \quad (15)$$

Then:

$$COA_{th}^{W_0} = 1 + \frac{n_R(h_1^n - h_3^n)}{n_{c \rightarrow a}(h_c^n - h_a^n)} = 1 + COP_{th}^{W_0} \quad (16)$$

$$COA_{ex}^{W_0} = \frac{COA_{th}^{W_0}}{COA_C^{W_0}} \quad (17)$$

These values are compared for different pairs of working fluids and for several variants of CHV3T process. The next section gives additional details about such computations and allows comparing the different solutions between them.

3.2.1. CHV3T variants implementing internal energy recovery

During the different phases of CHV3T – W_0 process, one fraction of the working fluid internal energy can be recovered instead of being dissipated through the condenser of the motor cycle.

The W_L and W_G variants offer two different solutions for increasing the thermodynamic efficiency of the cycle.

CHV3T – W_L cycle: When two W_0 cycles operate together in phase opposition, the cylinders C_{TM} and $C_{TR'}$ are connected during the ε phase. Consequently, the high pressure inside C_{TM} increases the low pressure in $C_{TR'}$ as far as an intermediate pressure P_m . These additional expansion/compression step is pictured on the Mollier diagram below (states 1_m and c_m) and lead to a better efficiency.

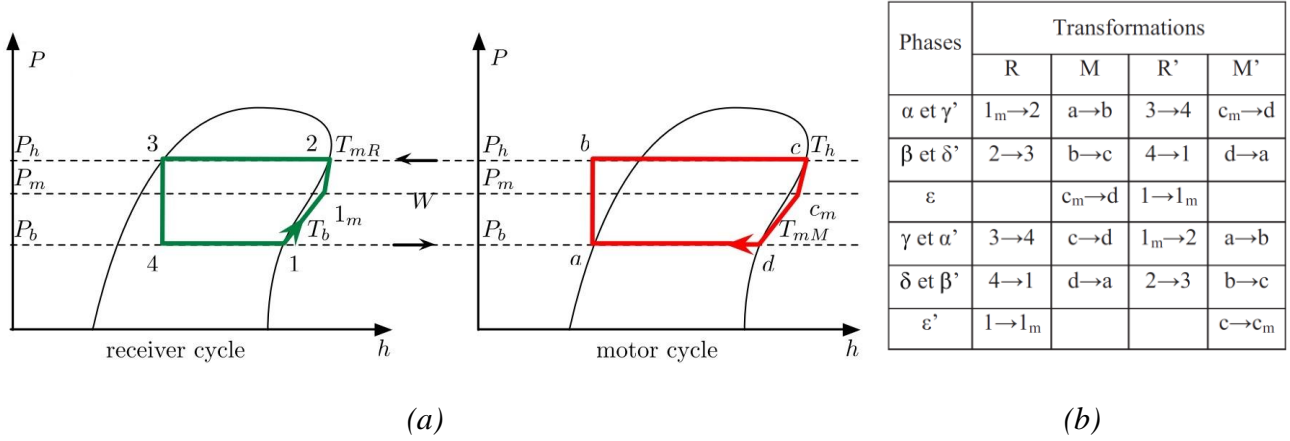


Fig. 6. Motor and receptor Mollier diagram of CHV3T cycle in W_L variant (a) transformations during the different phases (b)

The equations modeling the theoretical and quasi-static performances of the W_L variant are:

COP computation:

$$COP_C^{WL} = \frac{T_b(T_h - T_{mM})}{T_h(T_{mR} - T_b)} \quad (18)$$

$$COP_{th}^{WL} = \frac{v_{cm}^n (h_1^n - h_4^n)}{v_1^n (h_c^n - h_a^n)} \quad (19)$$

COA computation:

$$COA_C^{WL} = 1 + COP_C^{WL} \quad (20)$$

$$COA_{th}^{WL} = 1 + COP_{th}^{WL} \quad (21)$$

CHV3T – W_G cycle: this variant consists in recovering the expansion work through the gaseous phase of receptor or motor fluids, and not thanks to the hydraulic liquid transfer. To do so, an additional receiving bottle is added to the driving and receiving cycles and is used for injecting high-pressure fluid inside cylinders during the phase of their pressurization. The main advantage of the W_G variant is into the control command of the system.

The CHV3T – W_{LG} and CHV3T – W_{GL} cycles hold concurrently the advantages of both W_G and W_L cycles, but the sequences of recovery phases are different. For the first variant, the recoveries of work start with the hydraulic transfer and end with the gas phase. For the second variant, these both sequences are reversed. Despite of better efficiency, both variants suffer from an important complexity: in particular, the phase management of the whole cycle becomes really complicated.

3.3 CAPILI Cycle

In order to improve the efficiency of the electricity production, the working conditions need to be changed in comparison to the operating conditions of CHV3T cycle. An optimal heat source temperature has to be set in order to maximize the exergetic efficiency of the system made of CAPILI system and the solar collectors. Indeed, when the evaporation temperature increases, the Carnot efficiency of the engine cycle increases while the solar collector efficiency decreases.

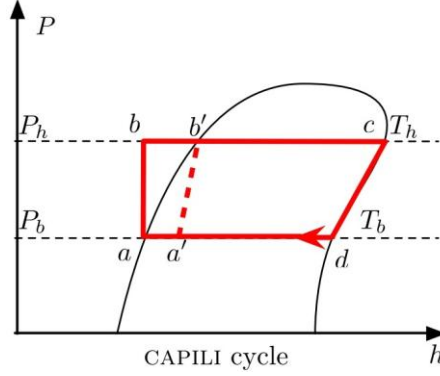


Fig. 7. Mollier diagram of first (a-b-c-d) and second type (a'-b'-c-d) of CAPILI Cycle.

Carnot and exergetic efficiency can be computed thanks to:

$$\eta_c = 1 - \frac{T_b}{T_h} \quad (22)$$

$$\eta_{ex} = \frac{\eta_{CPL}}{\eta_c} \quad (23)$$

3.3.1 CAPILI (1st type)

In this version, the efficiency of the CAPILI cycle is given by :

$$\eta_{CPL^1} = \frac{|\Sigma w|}{q_h} = \frac{(h_c - h_d) - (h_b - h_a)}{h_c - h_b} \quad (24)$$

3.3.2. CAPILI (2nd type)

In this second version, the compression (a'-b') of the working fluid is operated in biphasic state. Consequently, an additional work is required to compress the fluid from P_b to P_h , but the thermal load of the evaporator is greatly reduced, enhancing the final efficiency in comparison to the first type of CAPILI cycle. The efficiency equation is:

$$\eta_{CPL^2} = \frac{(h_c - h_d) - (h_{b'} - h_{a'})}{h_c - h_{b'}} \quad (25)$$

3.4. Selecting the pair of working fluids

The selection of the working fluids leads to large differences on the performances of the thermo-hydraulic process. This topic has already been studied on different articles [14], [15]. The main difficulty of the CHV3T cycle is a pair of fluids able to work together between the receptor and motor cycles. They have to fulfil several criteria:

- compatibility of operating pressures and temperatures of both working fluids, (Fig 8)
- environmental friendly fluid with null ODP (Ozone Depletion Potential), and low GWP (Global Warming Potential).
- lack of toxicity and corrosiveness for safety purpose.

Among the different family of working fluid, such as CFC, HFC, Hydrocarbon or HFE, CoolProp and RefProp libraries offer the possibilities to test a very large selection of working fluids.

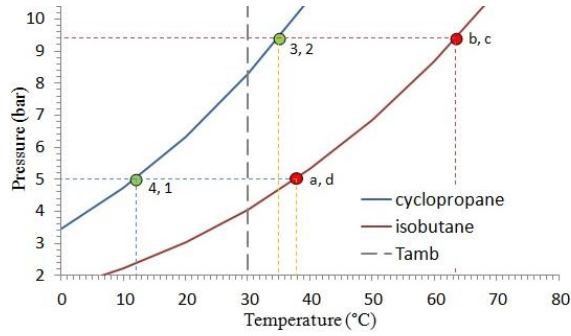


Fig. 8. Pressure-Temperature diagram of two selected fluids for the CHV3T application

An algorithm has been implemented to test all the fluids taking part in the different databases. The heat exchanger efficiencies (ϵ_{gl} and ϵ_{ll}) are respectively 0.7 and 0.65 with a pinch (ΔT_p) of 1.5°C and irradiance is 800W/m². The fluids not satisfying the operating conditions are not further considered in the simulation. The performances of different pairs of working fluids have been computed in order to select the one that achieve the best heat and cold production, in term of global COP ($COP_{th} \cdot \eta_{coll}$) and global COA ($COA_{th} \cdot \eta_{coll}$), it take account of the solar collector efficiency to calculate the full system efficiency. Each solution made of a fluid pair and a solar collector is simulated. Around 30 solar collector outcome of different manufacturer are tested. Its performances are plotted on Figure 9(a), for the CHV3T-W₀ variant. Two different kinds of solution are plotted: the ones with small dots are the fluid pairs including at least one fluid that does not match with the ODP, GWP or toxicity requirement, whereas the ones with large dots are suitable solutions. This graph highlights that several optimal solutions exist, depending on the designer will to give advantages to the heat or cold production.

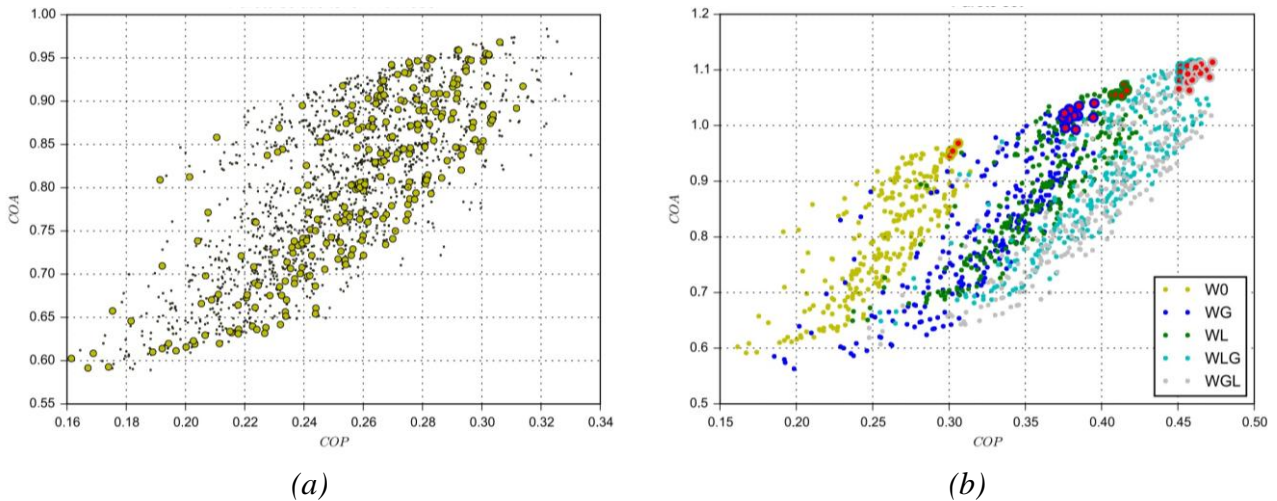


Fig. 9. Global efficiencies of CHV3T-W₀ for different fluids and solar collectors. (a) Global efficiencies of all CHV3T variants with different fluids and solar collectors (b)

The same approach is applied to other variants of CHV3T cycle and the results are displayed on Figure 9 (b). It clearly underlines the efficiency leap between each technological variant: however, it is worth noting that increasing the system complexity is required to do so. The five most interesting working fluid pairs have the advantage of a really poor GWP, in spite of their flammability since they belong to the hydrocarbons family: Cyclopropane/IsoButane, Propyne/n-Butane, Propyne/trans-2-Butene, Cyclopropane/1-Butene, Cyclopropane/IsoButene.

If the use of flammable fluids is not possible, refrigerant fluids from the 4th generation (HFO) may be carried since some pairs are able to reach good performances. The fluid selected for the CHV3T motor cycle is also used within CAPILI cycle: consequently, the motor fluid must insure good performances for electricity production and lead to a trade-off during the selection process.

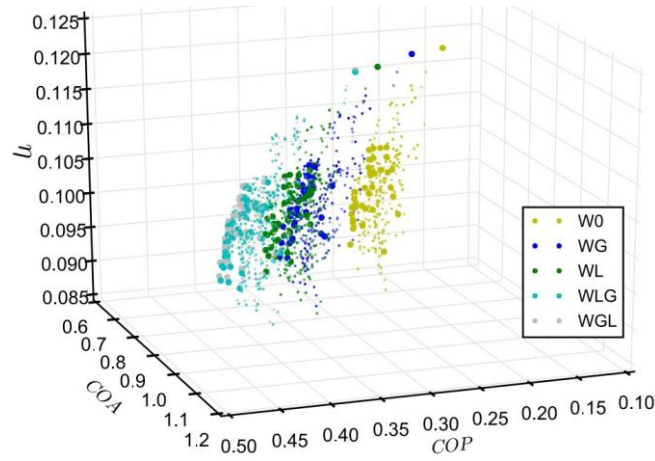


Fig. 10. Global efficiencies of CHV3T- W_G and CAPILI 1st type for different fluids and collectors.

Three examples are given in the following table. T_h and T_b are the evaporation and condensation temperatures, the collector efficiency are evaluated for vacuum solar collector found in the industry and for irradiance of 800W/m². The CHV3T- W_G results are given in the Table1 for three different pairs of fluid.

Table 1. Performances of CHV3T- W_G with three different pairs of fluid.

Fluid Couple	R134a/R236fa	R1234yf/R600a	Cyclopropane/R600a
T_{ext} (winter/summer)		17°C/30°C	
T_h	65.8°C	61.2°C	63.4°C
T_b	12°C	12°C	12°C
$\Delta P = P_h - P_b$	4.44 bar	4.3 bar	4.39 bar
η_{coll} (winter/summer)	0.65/0.68	0.66/0.69	0.66/0.69
Internal cycle efficiencies :			
COP_c / COA_c	0.93 / 1.93	0.97 / 1.97	0.94 / 1.94
COP_{th} / COA_{th}	0.51 / 1.51	0.55 / 1.55	0.57 / 1.57
COP_{ex} / COA_{ex}	0.55 / 0.78	0.57 / 0.79	0.6 / 0.81
Global efficiencies [$(COP_{th}$ or $COA_{th}) \cdot \eta_{coll}$] :			
COP / COA	0.351 / 0.991	0.382 / 1.032	0.391 / 1.035

In the Table 2, the working fluid of the motor cycle is used to set into motion a 1st type CAPILI cycle in the same operating conditions given in Table 1. T_b temperature is increased to correspond at the average external temperature and T_h temperature is also increased to reach a better efficiency

Table 2. Performances of CAPILI 1st type with three different pairs of fluid.

Fluid Couple	R134a/R236fa	R1234yf/R600a	Cyclopropane/R600a
T_{ext}		23.5°C	
T_h		80°C	
T_b		18.5°C	
$\Delta P = P_h - P_b$	10.29 bar	10.55 bar	10.55 bar
η_{coll}	0.68	0.68	0.68
Internal cycle efficiencies :			
η_c	0.174	0.174	0.174
η_{th}	0.139	0.143	0.143
η_{ex}	0.799	0.823	0.823
Global efficiency [$\eta_{th} \cdot \eta_{coll}$] :			
η	0.094	0.097	0.097

The electrical efficiency of the whole system is the product of the hydraulic/mechanical/electrical conversion chain efficiency with the global efficiency.

4. Performance comparison and discussion

This study shows that both CHV3T and CAPILI processes have a valuable potential with satisfying exergetic efficiency for heat, cold and electricity. Contrary to the current mCHP processes that produced heat and electricity at the same time, this system is able to adjust its production in function of the needs and to the available resources. Therefore, the designer has the possibility to choose between a decentralized production or a cogeneration approach.

However, the quasi-static hypothesis assumed to compute the different exergetic efficiencies should be revoked and a dynamic simulation could lead to a more accurate understanding of the thermodynamic phenomena. In particular, this approach should allow evaluating the pressure loss and the thermal inertia of different components. The hydraulic/mechanic/electric conversion chain also requires a dynamic simulation to accurately evaluate the efficiency evolution during the phases involving a variable pressure difference.

This proceeding also underlines that W_G variant of CHV3T and 1st type CAPILI is a suitable trade-off between the performances and the process complexity. It also seems to be the best cost-effective choice according to the operating and working conditions of the fluids. To that purpose, the algorithm developed in order to select the different pairs of fluids helps finding a trade-off between the different variables. CHV3T- W_G also appears as an attractive alternative for solar heating and cooling technologies due to its ability to use low temperature driving heat source (65°C) like flat plate collectors. With a global COP ($COP_{th} \cdot \eta_{coll}$) of 0.57 and COA of 1.57, this process is competitive on the domestic heat and cold production market.

The electricity production performances are more reduced with approximately 6% annual efficiency due to the low temperature difference between cold and heat sources (18.5°C/80°C) and a realistic average irradiance. However, the CAPILI process exhibits a good exergetic efficiency, which is above 80% for the internal cycle. With an hydraulic turbine especially designed to operate under the CAPILI operating conditions, a better efficiency than ORC could be reached due to the low quantity of irreversibilities. A modeling of the full processes is now under development by using the Modelica language: the main objective is to provide a design tool for sizing a small-scale pilot of 1kWe.

Acknowledgments

This study has supported by SATT-AxLR, an accelerating and maturing technology company, under the TRIGETHYSOL project (<http://trigethysol.com/>)

Nomenclature

Symbol		q	specific heat, J/kg
BS	receiver	\dot{q}	heat power, W
C	condenser	T	temperature, K
COP	coefficient of performance	w	specific work, J/kg
COA	coefficient of amplification	\dot{w}	power, W
CT	transfer cylinder		
E	evaporator	Greek symbols	
G	solar irradiance, W/m ²	Δ	difference
h	specific enthalpy, J/kg	ε	heat exchanger effectiveness
h^n	molar specific enthalpy, J/mol	η	efficiency
HT	hydraulic turbine	η_0	optical efficiency
n	amount of substance, mol	v	specific volume, m ³ .kg ⁻¹
P	pressure, Pa	v^n	molar volume, m ³ .mol ⁻¹

Subscripts and superscripts

1, 2, 3, 4	particular points in Mollier diagram relative to receiver cycle	gl	gaseous/liquid
a, b, c, d	particular points in Mollier diagram relative to engine cycle	h	hot
b	cold	in	inlet
C	Carnot	ll	liquid/liquid
coll	collector	mM	medium Motor cycle
CPL ¹	CAPILI fist type	mR	medium Reverse cycle
CPL ²	CAPILI second type	out	outlet
ex	exergetic	R	receiver cycle
ext	ext	M	engine cycle
f1	heat transfer fluid inlet	th	internal thermodynamic
f2	heat transfer fluid outlet	wf	working fluid
		wfi	working fluid intermediary
		wf1	working fluid inlet
		wf2	working fluid outlet

References

- [1] « IPCC - Intergovernmental Panel on Climate Change ». Available at: <http://www.ipcc.ch/index.htm>. [accessed: 16.02.2015].
- [2] « 2030 framework for climate and energy policies - European Commission ». Available at: http://ec.europa.eu/clima/policies/2030/index_en.htm. [accessed: 16.02.2015].
- [3] H. I. Onovwiona et V. I. Ugursal, « Residential cogeneration systems: review of the current technology », *Renew. Sustain. Energy Rev.*, vol. 10, n° 5, p. 389-431, oct. 2006.
- [4] M. M. Maghanki, B. Ghobadian, G. Najafi, et R. J. Galogah, « Micro combined heat and power (MCHP) technologies and applications », *Renew. Sustain. Energy Rev.*, vol. 28, p. 510-524, déc. 2013.
- [5] B. Aoun, « Micro-cogénération pour les bâtiments résidentiels fonctionnant avec des énergies renouvelables », École Nationale Supérieure des Mines de Paris, 2008.
- [6] J. Demierre, D. Favrat, J. Schiffmann, et J. Wegele, « Experimental investigation of a Thermally Driven Heat Pump based on a double Organic Rankine Cycle and an oil-free Compressor-Turbine Unit », *Int. J. Refrig.*, vol. 44, p. 91-100, août 2014.
- [7] S. Hargreaves « Patent EP2105610A1 - Method for converting thermal energy into mechanical work » sept. 2009. Available at: <http://www.google.bj/patents/EP2105610A1?cl=en&hl=fr>. [accessed: 16.02.2015].
- [8] P. Van De Loo, D. R. Barduca « Patent 20100300097 - HEAT ENGINE » déc.2010. Available at: <http://www.faqs.org/patents/app/20100300097>. [accessed: 16.02.2015].
- [9] H. Semmari, D. Stitou, et S. Mauran, « A novel Carnot-based cycle for ocean thermal energy conversion », *Energy*, vol. 43, n° 1, p. 361-375, juill. 2012.
- [10] S. Mauran, M. Martins, D. Stitou, et H. Semmari, « A novel process for engines or heat pumps based on thermal-hydraulic conversion », *Appl. Therm. Eng.*, vol. 37, p. 249-257, mai 2012.
- [11] M. Martins, S. Mauran, D. Stitou, et P. Neveu, « A new thermal-hydraulic process for solar cooling », *Energy*, vol. 41, n° 1, p. 104-112, mai 2012.
- [12] S. Quoilin, M. V. D. Broek, S. Declaye, P. Dewallef, et V. Lemort, « Techno-economic survey of Organic Rankine Cycle (ORC) systems », *Renew. Sustain. Energy Rev.*, vol. 22, p. 168-186, juin 2013.
- [13] « Solar Keymark ». Available at: <http://www.estif.org/solarkeymarknew/index.php>. [accessed: 16.02.2015].
- [14] J. Bao et L. Zhao, « A review of working fluid and expander selections for organic Rankine cycle », *Renew. Sustain. Energy Rev.*, vol. 24, p. 325-342, août 2013.
- [15] G. Qiu, « Selection of working fluids for micro-CHP systems with ORC », *Renew. Energy*, vol. 48, p. 565-570, déc. 2012.